Mode Switching in a Gyrotron with Azimuthally Corrugated Resonator

G. S. Nusinovich, O. V. Sinitsyn, and T. M. Antonsen, Jr.
IREAP, University of Maryland, College Park, Maryland 20742-3511, USA
(Received 15 December 2006; published 14 May 2007)

The operation of a gyrotron having a cylindrical resonator with an azimuthally corrugated wall is analyzed. In such a device, wall corrugation cancels the degeneracy of the modes with azimuthally standing patterns. The coupling between these modes depends on the radius of electron beam. It is shown that such a gyrotron can be easily switched from one mode to another. When the switching is done with the repetition frequency equal to the rotational frequency of magnetic islands, this sort of operation can be used for suppression of neoclassical tearing modes in large-scale tokamaks and stellarators.

DOI: 10.1103/PhysRevLett.98.205101 PACS numbers: 84.40.Ik, 52.59.Rz

High-power, millimeter-wave gyrotron oscillators and amplifiers are presently used for numerous applications, which include plasma heating [1] and radars [2]. Normally, gyrotron oscillators operate in a single mode. Here we consider a gyrotron with a resonator whose wall is azimuthally perturbed such that counter-rotating modes are coupled together. In this situation, composite modes are formed. The coupling between these modes depends on the radius of the electron beam. It is shown below that at certain beam positions, the gyrotron can be easily switched from one mode to the other. This allows one to provide rapid changes in gyrotron operation by using a low-power, short-pulse driver.

In a conventional cylindrical (or coaxial) resonator, nonsymmetric (i.e., having a nonzero azimuthal index m, $\exp[\pm im\varphi]$) waves rotating azimuthally in opposite directions, as well as standing waves with azimuthal distribution $\cos m\varphi$ or $\sin m\varphi$ are degenerate. A beam of electrons rotating in the applied magnetic field being a gyrotropic medium breaks the degeneracy of rotating waves. Thus, such a beam excites one of these waves, the one that is more strongly coupled to the beam [3]. In turn, when the resonator wall is azimuthally corrugated, as shown in Fig. 1, and the number of these corrugations is twice the azimuthal index m of the operating mode, the corrugation provides the coupling between two rotating waves and, hence, leads to formation of standing wave patterns. Such cosine and sine modes have different frequencies. Their frequency separation is $2\Delta\omega$, where [4]

$$\frac{\Delta\omega}{\omega} = \frac{d}{2R_w}\frac{\nu^2+m^2}{\nu^2-m^2}. \qquad (1)$$

In (1), d is the corrugation depth, R_w is the unperturbed radius, ν is the eigennumber of the operating mode, and $\omega$is the mode frequency in the absence of corrugations. This situation is similar to the coupling between two waves propagating in opposite directions in a dielectric medium with spatially periodic modulations [5]. When both effects (the effect of the electron beam and the effect of the wall perturbation) are of the same order, normal modes represent superpositions of either rotating or standing waves. The interaction between these modes and the possibility to switch the gyrotron operation from one mode to another are analyzed below. We consider the case when the frequency separation $2\Delta\omega$ is much smaller than the cyclotron resonance band and, hence, both waves can operate with the same efficiency.

Omitting the details of derivation, which are similar to those described elsewhere [6,7], equations for the interaction between the two rotating waves with complex amplitudes $A_\pm$ can be given in the quasilinear approximation as

$$\frac{dA_\pm}{dt} + \frac{\omega}{2Q}A_\pm = -i\Delta\omega A_\mp + \omega I\frac{1}{2\pi}\int_0^{2\pi} J_{m\mp s}(\xi) \times e^{-i(s\mp m)\varphi}\{\alpha A - \beta A|A|^2\}d\varphi, \qquad (2)$$

where Q is the quality factor for the two modes, I is the normalized beam current defined in [6], $A(\varphi) = J_{m-s}(\xi)e^{-i(m-s)\varphi}A_+ + J_{m+s}(\xi)e^{i(m+s)\varphi}A_-$ represents the

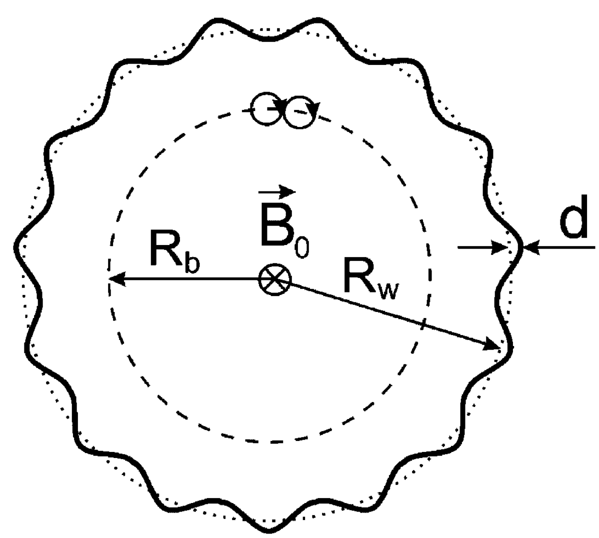

FIG. 1. Cross-section of the interaction space in the gyrotron with a thin annular electron beam and a resonator having an azimuthally corrugated wall.

local amplitude of the azimuthally dependent field component that resonantly interacts with gyrating electrons. Here, the coupling coefficients $J_{m\pm s}(\xi)$ are ordinary Bessel functions, s is the cyclotron resonance harmonic, and $\xi = \omega R_b/c$ where R_b is the beam radius. The complex coefficients α and β describe the linear interaction of the beam with the fields and the saturation, respectively. These quantities give rise to a complex frequency shift of the individual uncoupled modes, proportional to the beam current, $\delta\omega_\pm = i\omega I J^2_{m\mp s}(\xi)\{\alpha A_\pm - \beta A_\pm J^2_{m\mp s}(\xi)|A_\pm|^2\}$. The real parts of α and β determine the current required to start oscillations of the uncoupled modes, $I_{st,\pm} = 1/2Q\mathrm{Re}(\alpha)J^2_{m\mp s}(\xi)$, and the saturated amplitude of the uncoupled modes, $|A_\pm|^2 = \mathrm{Re}(\alpha)(1 - I_{st,\pm}/I)/\mathrm{Re}(\beta)J^2_{m\mp s}(\xi)$. The imaginary parts determine the beam induced frequency shift. These coefficients depend on the axial structure of modes and the detuning between the cavity frequency and the s-th harmonic of the electron cyclotron frequency [6].

The difference in electron interaction with the two rotating modes can be characterized by the ratio of the Bessel functions, $q = J^2_{m+s}(\xi)/J^2_{m-s}(\xi)$. The dependence of this ratio on the radius of a thin electron beam is illustrated by Fig. 2. Here, Fig. 2(a) shows the dependence of functions $J^2_{m\pm s}(\omega R_b/c)$ on the beam radius for the $\mathrm{TE}_{22,6}$-mode operating at the fundamental cyclotron resonance (this mode is typical of those used in MW-level gyrotrons [8]). Figure 2(b) shows corresponding dependence of the q ratio on beam radius.

If one performs the average over angle φ in (2), one obtains

$$\frac{dA_\pm}{dt} + \frac{\omega}{2Q}A_\pm = -i\Delta\omega A_\mp + \omega I J^2_{m\mp s}\{\alpha - \beta[J^2_{m\mp s}|A_\pm|^2 + 2J^2_{m\pm s}|A_\mp|^2]\}A_\pm. \quad (3)$$

So, similar to a classical two-mode rf oscillator [9], there is a strong cross-saturation effect (the term with the factor 2); i.e., one rotating mode strongly suppresses another [6].

Equation (3) applies to the amplitudes of the two counter-rotating waves. When the corrugations are present, it is more appropriate to represent the field as a superposition of standing waves, $A_\pm = A_1(t)e^{-i\Delta\omega t} \pm A_2(t)e^{i\Delta\omega t}$. Here, $A_{1,2}$ are the complex amplitudes of standing waves, which in the absence of the beam have frequency shifts $\pm\Delta\omega$ (1) relative to the case of a smooth walled resonator. Evolution equations for these amplitudes are then obtained by taking the sum and difference of the two versions of (3) and substituting for $A_\pm$.

We now focus on the case when the frequency shift $\Delta\omega$ is large compared with the inverse cavity decay time $\omega/2Q$. In this case, the phases of the two standing modes vary rapidly in time compared with the variation of the amplitudes; so we may average the equation for the standing mode amplitudes over a time period $2\pi/\Delta\omega$. The result is

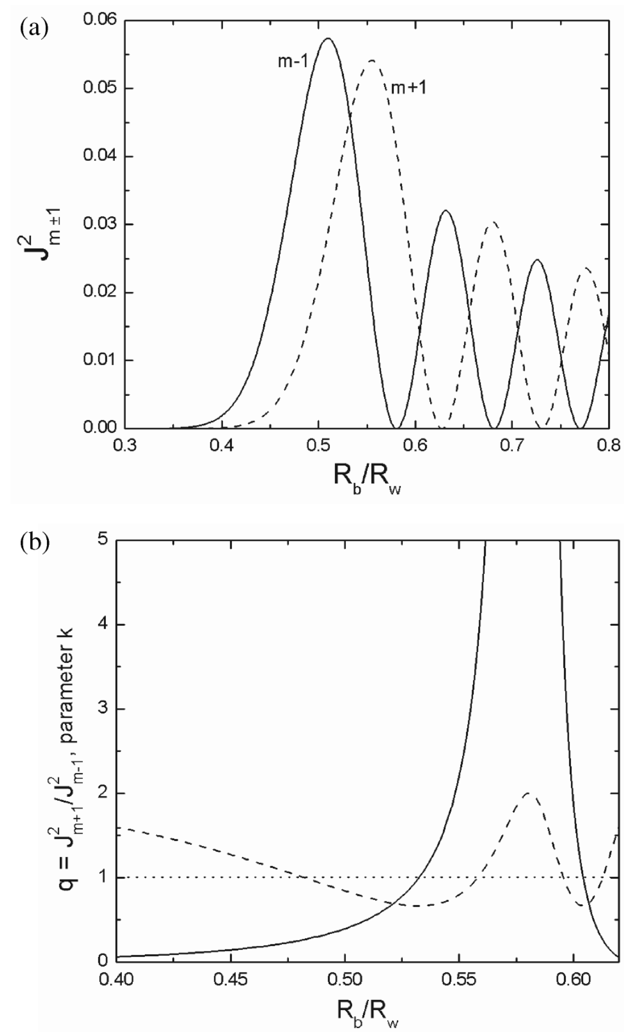

FIG. 2. (a) Dependence of coefficients characterizing the coupling of a thin annular electron beam to co- and counter-rotating $\mathrm{TE}_{22,6}$-waves on the beam radius. (b) Dependence of the q ratio (solid lines) and the parameter k characterizing the coupling between modes (dashed line) on the beam radius for the $\mathrm{TE}_{22,6}$-mode.

$$\frac{dA_{1,2}}{dt} + \frac{\omega}{2Q}A_{1,2} = \omega I\bar{J}^2\{c_1\alpha - \beta\bar{J}^2[c_2|A_{1,2}|^2 + c_3|A_{2,1}|^2]\}A_{1,2} + \omega S_{dr,1,2} \quad (4)$$

where $c_1 = (q^{1/2} + q^{-1/2})/2$, $c_2 = (q + q^{-1} + 4)/2$ and $c_3 = q + q^{-1}$, and $\bar{J}^2 = J_{m+s}(\xi)J_{m-s}(\xi)$. The last term in the right hand side represents the possible presence of injected signals at the frequencies corresponding to the two standing modes. We will consider the effect of injected signals on the mode dynamics subsequently. Coefficients c_2 and c_3 describe the self and cross-saturation terms. When the cross saturation is smaller than the self-saturation, the coupling between modes is weak, as in gas lasers [10], and the device exhibits stable two-mode oscillations, while otherwise the coupling is strong and only single-mode oscillations are stable, as in a classical rf oscillator [9]. The condition for weak coupling ($c_3 < c_2$) is [4]

$$2 - \sqrt{3} \le q \le 2 + \sqrt{3}. \qquad (5)$$

In Fig. 2(b), the dependence of the q ratio on the beam radius is shown for the gyrotron operating in the $TE_{22,6}$-mode. Also shown, by a dashed line, is the ratio $k = c_3/c_2 = 2(q + q^{-1})/(q + 4 + q^{-1})$. Strong coupling corresponds to $k > 1$. For conventional gyrotrons, this ratio of corresponding cross-saturation terms to self-saturation ones, which is different from those in [4], is equal to 2. As it follows from Fig. 2(b), the most convenient way to control the value of k is to position the beam in the near-caustic region ($R_0 = (0.46 - 0.48)R_w$) where the radial dependence of Bessel functions is rather smooth. Then the operating characteristics can be modified if k is chosen to be close to the boundary between weak and strong coupling. For instance, a gyrotron can be easily switched to operation from one mode to another in this regime using an injected signal, as shown below. As follows from Ref. [11], the gyrotron efficiency in this case is equal to 3/4 of the efficiency of a conventional gyrotron.

To reduce the number of parameters, Eqs. (4) can be rewritten as

$$\frac{d\bar{A}_{1,2}}{d\tau} = \bar{A}_{1,2}\{1 - \bar{A}_{1,2}^2 - k\bar{A}_{2,1}^2\} + A_{dr,1,2}. \qquad (6)$$

In (6), we introduced the slowly variable time $\tau = \sigma(\omega t/2Q)$, which is normalized to the increment $\sigma = (I/I_{st}) - 1$, the mode amplitudes $\bar{A}_{1,2} = \sqrt{\hat{\beta}}A_{1,2}$ are normalized to the saturation coefficient $\hat{\beta} = (IQ/\sigma) \times (\bar{J}^2/2)^2 \mathrm{Re}(\beta)c_2$, and the normalized amplitude of the drive signal is $A_{\mathrm{dr}} = \sqrt{\hat{\beta}}(2QS/\sigma)$. The coefficients α and β are both taken to be real.

Numerical results from (6) are shown in Fig. 3. Here, we have set the source for mode 1 to zero and the source for mode 2 to be a real quantity implying that the frequency of the source coincides with the frequency of mode 2. Figure 3(a) illustrates a typical time evolution of both amplitudes. It shows initial operation of a gyrotron at the first mode in the absence of a driver. When the driver is turned on, the switching process starts. This process results in the switching to the second mode, which remains stable after turning the driver off. For a 110-170 GHz gyrotron having the resonator with the quality factor of 10^3, this normalized switching time corresponds to the time interval less than 100 ns. When the drive amplitude exceeds its critical value only slightly, the switching may take a longer time.

Figure 3(b) shows the critical value of the drive amplitude required for switching the oscillator from the first mode to the second as the function of the parameter k. As expected, the critical value of the drive amplitude required for switching the device increases with the departure from the boundary ($k = 1$) between the weak ($k < 1$)

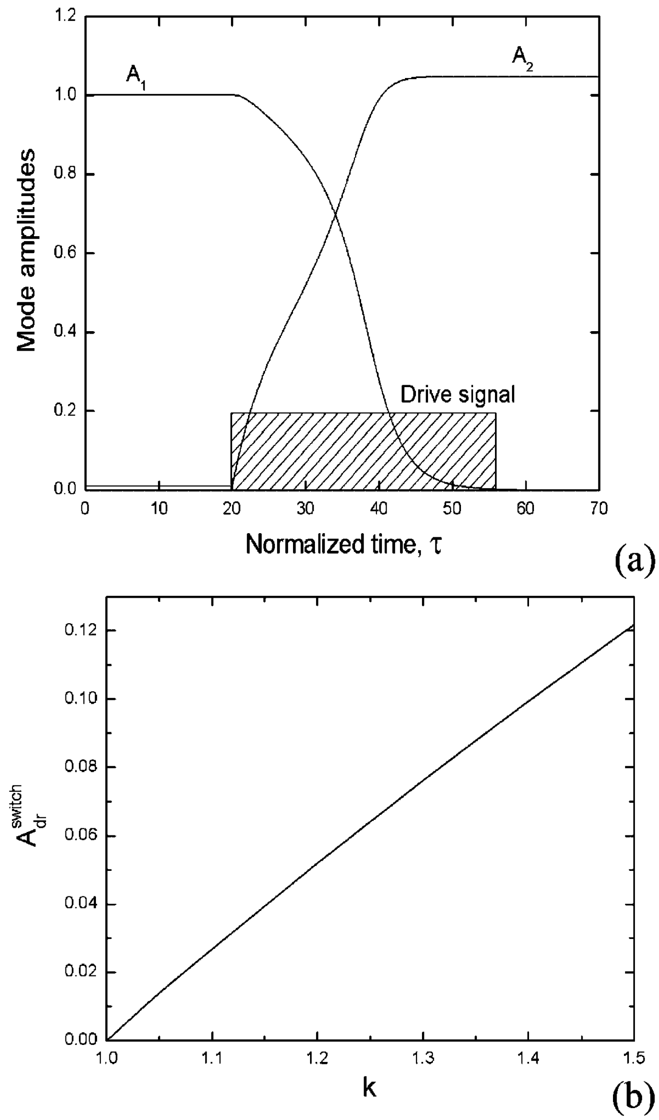

FIG. 3. (a) Typical evolution of mode amplitudes in the process of switching from the first mode to the second; (b) critical switching amplitude of the drive signal as the function of the parameter k characterizing the excess of the cross-saturation over the self-saturation.

and strong ($k > 1$) coupling. To interpret the value of the normalized amplitude of the drive signal required for switching, one should analyze the normalization of this amplitude given after (6) and take into account that the original drive term S_{dr} in (4) relates to the power of a driver as [12] $(2QS)^2 = 4IQ(Q/Q_{\mathrm{cpl}})(P_{\mathrm{dr}}/P_{b\perp})$. Here, Q_{cpl} is the coupling Q factor, $P_{b\perp}$ is the beam power associated with electron gyration. As follows from these relations, the drive power required for switching the gyrotron is proportional to the squared switching amplitude shown in Fig. 3(b) and to the power of gyrotron radiation. The latter fact agrees with the Adler's conclusion [13] that the drive power required for phase locking of an oscillator is proportional to the power of oscillations. As shown in Fig. 3(b), the critical value of the drive amplitude increases linearly as $(k-1)$ grows. This means that the drive power required for switching in the gyrotron with an azimuthally corrugated resonator can be $(k-1)^2$ times smaller than in conventional gyrotrons where $k=2$.

To estimate the drive power with the use of Fig. 3(b), we took a set of typical parameters for a 1 MW gyrotron: 90 kV, 40 A electron beam with the orbital-to-axial velocity ratio of 1.3, $TE_{22,6}$-mode, total Q factor of 1600, ratio of the cavity length to the wavelength equal to 6. We also assumed that the axial distribution of the rf field in the resonator is constant, the driver is critically coupled to the cavity, the beam location corresponds to the maximum of beam coupling to the desired mode and the q ratio is equal to 0.2 that is close to the boundary between strong and weak coupling given in (5) by $2-\sqrt{3}$. Then, the drive power remains dependent on the linear growth rate α and the saturation term β, which can vary with the magnetic field when the beam parameters are fixed. If we assume $\hat{\beta}=1$, then we find that for switching a conventional gyrotron from one mode to another, it is necessary to apply 60 kW drive power, while in the case of the gyrotron with azimuthally corrugated resonator and $k=1.1$, it is enough to use about 1 kW only. Note that in the case of using additional resonator for electron prebunching (as in gyroklystrons), the required drive power can be much lower.

In recent years, there is a strong interest in using gyrotrons for suppression of neoclassical tearing modes (NTMs) [14]. For the most efficient use of gyrotrons for this purpose in large tokamaks and stellarators (such as ITER or W7-X), it is desirable to have gyrotrons operating in a modulated regime with the modulation frequency corresponding to the rotational frequency of magnetic islands (a so-called AC method of NTM stabilization [15]). To realize such low-frequency modulation of gyrotron radiation (rotational frequency of magnetic islands is on the order of 10 kHz), it was proposed [16] to use a gyrotron operating in a single mode with a periodic modulation of either the mod-anode voltage (in the case of triode-type electron guns) or the resonator voltage (in the case of gyrotrons using diode type guns and depressed collectors). Such a gyrotron should be supplemented by a narrow-band frequency diplexer capable of directing the gyrotron wave beam to one of two output channels [16]. To keep the gyrotron single-mode efficiency high, it is necessary to modulate the frequency in the scale much smaller than the width of resonance curve of a given mode that imposes some limitations on the design of a narrow-band diplexer [16].

The use of a gyrotron with a resonator having an azimuthally corrugated wall offers a new possibility for this application. Indeed, the corrugation depth can be adjusted for the frequency separation between two standing modes to be large enough for reliable operation of the frequency diplexer [16]. Then, when the beam position corresponds to the q ratio slightly outside the boundaries of weak coupling region (5), the coupling between two modes is still strong, but the device can be switched from operation in one mode to another with the use of a low-power driver. To switch the device back to the first mode, the next pulse of a driver should excite the first mode.

The results obtained demonstrate that gyrotrons with azimuthally corrugated walls controlled by a two-frequency, short-pulse driver operating with the repetition frequency equal to the rotational frequency of magnetic islands can be used for the AC suppression of NTM modes in conjunction with the frequency diplexer [16].

This work is supported by the Office of Fusion Energy of the US Department of Energy. The authors are indebted to M. I. Petelin and J. Lohr for valuable discussions.

[1] K. Felch, H. Huey, and H. Jory, J. Fusion Energy **9**, 59 (1990); M. Thumm, Plasma Phys. Controlled Fusion **45**, A143 (2003).

[2] K. Felch, B. G. Danly, and H. R. Jory *et al.*, Proc. IEEE **87**, 752 (1999).

[3] G. S. Nusinovich, O. Dumbrajs, and B. Levush, Phys. Plasmas **2**, 4621 (1995).

[4] G. S. Nusinovich, Radio Eng. Electron. Phys. **19**, 152 (1974).

[5] V. S. Butylkin, A. E. Kaplan, Yu. G. Khronopulo, and E. I. Yakubovich, *Resonant Nonlinear Interactions of Light and Matter* (Springer-Verlag, Heidelberg, 1989), p. 126; M. I. Rabinovich, Radiophys. Quantum Electron. **17**, 361 (1974); M. Botton and A. Ron, Phys. Rev. Lett. **66**, 2468 (1991).

[6] G. S. Nusinovich, Int. J. Electron. **51**, 457 (1981); G. S. Nusinovich, *Introduction to the Physics of Gyrotrons* (Johns Hopkins University, Baltimore, 2004), Ch. 5.

[7] K. E. Kreischer and R. J. Temkin, in *Infrared and Millimeter Waves*, edited by K. J. Button (Academic, New York, 1983), Vol. 7, Ch. 8, p. 377.

[8] K. Felch *et al.*, IEEE Trans. Plasma Sci. **24**, 558 (1996); Y. Mitsunaka *et al.*, in *Proceedings of the 22nd Int. Conf. on IR, Wintergreen, Virginia, 1997*, edited by M. M. Waves, Conf. Digest, p. 19.

[9] B. Van der Pol, Proc. IRE **22**, 1051 (1934).

[10] W. E. Lamb, Phys. Rev. **134**, A1429 (1964).

[11] A. G. Luchinin and G. S. Nusinovich, Int. J. Electron. **57**, 827 (1984).

[12] V. S. Ergakov and M. A. Moiseev, Radiophys. Quantum Electron. **18** 89 (1975); G. S. Nusinovich, B. G. Danly, and B. Levush, Phys. Plasmas **4**, 469 (1997).

[13] R. Adler, Proc. IRE **34**, 351 (1946).

[14] H. Zohm *et al.*, Nucl. Fusion **39**, 577 (1999); G. Gantenbein *et al.*, Phys. Rev. Lett. **85**, 1242 (2000); A. Isayama *et al.*, Plasma Phys. Controlled Fusion **42**, L37 (2000); R. J. La Haye *et al.*, Phys. Plasmas **9**, 2051 (2002).

[15] H. Zohm *et al.*, Nucl. Fusion **41**, 197 (2001); H. Zohm *et al.*, in *Proceedings of the 21st IAEA Fusion Energy Conf., Chengdu, China* (IAEA, Trieste, 2006), paper EX/4-1Rb.

[16] W. Kasparek *et al.*, Fusion Sci. Technol. (to be published).